© 2014. Published by The Company of Biologists Ltd | Journal of Cell Science (2014) 127, 5317–5330 doi:10.1242/jcs.157610

RESEARCH ARTICLE

Ciliopathy proteins establish a bipartite signaling compartment in a *C. elegans* thermosensory neuron

Phuong Anh T. Nguyen[1], Willisa Liou[2], David H. Hall[3] and Michel R. Leroux[1,*]

ABSTRACT

How signaling domains form is an important, yet largely unexplored question. Here, we show that ciliary proteins help establish two contiguous, yet distinct cyclic GMP (cGMP) signaling compartments in *Caenorhabditis elegans* thermosensory AFD neurons. One compartment, a bona fide cilium, is delineated by proteins associated with Bardet–Biedl syndrome (BBS), Meckel syndrome and nephronophthisis at its base, and requires NPHP-2 (known as inversin in mammals) to anchor a cGMP-gated ion channel within the proximal ciliary region. The other, a subcompartment with profuse microvilli and a different lipid environment, is separated from the dendrite by a cellular junction and requires BBS-8 and DAF-25 (known as Ankmy2 in mammals) for correct localization of guanylyl cyclases needed for thermosensation. Consistent with a requirement for a membrane diffusion barrier at the subcompartment base, we reveal the unexpected presence of ciliary transition zone proteins where no canonical transition zone ultrastructure exists. We propose that differential compartmentalization of signal transduction components by ciliary proteins is important for the functions of ciliated sensory neurons.

KEY WORDS: cGMP signaling, Compartmentalization, Primary cilia, Sensory neuron, Thermotaxis, Transition zone

INTRODUCTION

Primary cilia are elaborate cellular organelles present on the surfaces of a large proportion of animal cells, including neurons, and function as sensory devices specialized for transducing various environmental stimuli (Berbari et al., 2009). Signaling components are often concentrated or dynamically incorporated within cilia, presumably to enhance and regulate signal capture and propagation (Corbit et al., 2005; Schneider et al., 2005; Simons et al., 2005). The diverse roles of primary cilia as 'cellular antennae' include the modulation of signaling pathways that perform essential roles in physiology and development. Hence, defects in components required for cilium formation and function are associated with a growing number of human disorders, collectively termed ciliopathies, which encompass developmental anomalies and loss of sensory modalities (Badano et al., 2006). Despite the recent efforts to study cilium-based signaling, our understanding of how signal transduction pathways are established and organized within cilia remains incomplete.

The second messenger cyclic GMP (cGMP) is widely utilized in biological systems, including sensory organs, and is present throughout the eukaryotic domain (Johnson and Leroux, 2010). cGMP is produced by guanylyl cyclases and broken down by phosphodiesterases (PDEs), whose activities can be modulated by G-protein-coupled receptors (GPCRs). cGMP can directly activate cyclic-nucleotide-gated (CNG) ion channels and cGMP-dependent protein kinases (PKGs), ultimately leading to various downstream effects, including activation of neurons. Recently, we highlighted the fact that cGMP signaling is confined to ciliated organisms (Johnson and Leroux, 2010). This correlation between cilia and the cGMP pathway suggests that ciliary proteins might be important in modulating cGMP signaling, and indeed this appears to be the case in vertebrate photoreceptors (Insinna and Besharse, 2008). In these cells, the connecting cilium (also known as transition zone) and outer segment represent a highly specialized cilium with an extensive membrane surface, where phototransduction is enabled through cGMP signaling. Retinal degeneration, often associated with mislocalization of cGMP signaling proteins, is a feature of many ciliopathies, such as in Bardet–Biedl syndrome (BBS) (Beales et al., 1999; Adams et al., 2007). However, other examples of ciliary proteins functioning in cGMP signaling are mostly lacking.

It is also unclear how different modules of ciliary proteins affect cGMP signaling. Many proteins disrupted in BBS patients assemble into a complex called the 'BBSome' (Nachury et al., 2007). This multimeric assembly functions with the small GTPase BBS3/ARL6 as a membrane-associated coat involved in trafficking ciliary cargoes (Jin et al., 2010). BBS proteins associate with the intraflagellar transport (IFT) machinery (Blacque et al., 2004; Ou et al., 2005; Ou et al., 2007), which uses motor proteins and accessory complexes to build and functionally maintain cilia (Silverman and Leroux, 2009; Sedmak and Wolfrum, 2011; Sung and Leroux, 2013). Signaling components that require BBS proteins for trafficking into (or out of) cilia include GPCR proteins, such as melanin-concentrating hormone receptor 1 (MCHR1), somatostatin receptor type 3 (SSTR3), dopamine receptor type 1 (D1) and rhodopsin (Nishimura et al., 2004; Berbari et al., 2008; Domire et al., 2011). Genetic studies implicate BBS proteins in cGMP signaling (Mok et al., 2011), but the molecular basis of their involvement remains undetermined. Another group of ciliary proteins linked to different ciliopathies, including nephronophthisis (NPHP), Meckel syndrome (MKS) and Joubert syndrome (JBTS), form part of a protein network present within the proximal-most region of the cilium (Reiter et al., 2012). This region, termed the transition zone, is characterized by Y-link structures connecting the axoneme with the membrane. The precise function of transition zone proteins is

[1]Department of Molecular Biology and Biochemistry, Simon Fraser University, Burnaby, BC V5A 1S6, Canada. [2]Department of Anatomy, Chang Gung University, Kwei-san Tao-yuan 333, Taiwan. [3]Department of Neuroscience, Albert Einstein College of Medicine, Bronx, New York, NY 10461, USA.

*Author for correspondence (leroux@sfu.ca)

Received 10 June 2014; Accepted 29 September 2014

Journal of Cell Science

Journal of Cell Science (2014) 127, 5317–5330 doi:10.1242/jcs.157610

currently unknown, but likely act as part of a gating mechanism that modulates the entry and exit of ciliary proteins (Rosenbaum and Witman, 2002; Craige et al., 2010; Williams et al., 2011; Sang et al., 2011; Garcia-Gonzalo et al., 2011). However, there is no evidence for transition zone protein involvement in cGMP signaling. So far, *Caenorhabditis elegans* DAF-25 (also termed CHB-3; ortholog of mammalian Ankmy2) is the only ciliary protein specifically associated with cGMP signaling (Fujiwara et al., 2010; Jensen et al., 2010). Disrupting DAF-25 results in the failure of two different guanylyl cyclase proteins (DAF-11 and GCY-12) to target to cilia in sensory neurons. In photoreceptors, Ankmy2 associates with the guanylyl cyclase GC1 (also known as GUCY2D) (Jensen et al., 2010). It remains unclear, however, what the mechanism of DAF-25 function is, and whether it represents a general modulator of guanylyl cyclase localization and function.

C. elegans represents an attractive system to study cilium-based cGMP signaling. Its cilia are exclusively found within an established subset of sensory neurons, and it has many guanylyl cyclases, some of which are known to be localized to cilia and are implicated in specific behaviors (Yu et al., 1997; Johnson and Leroux, 2010). A well-studied *C. elegans* behavior involving cGMP signaling is thermotaxis, the movement towards the cultivation temperature (Hedgecock and Russell, 1975). The bilateral ciliated AFD neurons are the major thermal sensors mediating this behavior (Mori and Ohshima, 1995), besides two other ciliated neurons, AWC and ASI (Kuhara et al., 2008; Beverly et al., 2011). Although their sensory modality is different, the thermosensory AFD neurons are suggested to be homologous to vertebrate photoreceptors, based on similarities at the level of transcription factors, molecular pathways, and complex morphology (Erclik et al., 2009). cGMP signaling components for AFD-mediated temperature sensing include the guanylyl cyclases GCY-8, GCY-18 and GCY-23, the CNG channels TAX-2 and TAX-4, and downstream modulators such as the protein kinase C TTX-4, the calcineurin A TAX-6 and the diacylglycerol kinase DGK-3 (Coburn and Bargmann, 1996; Komatsu et al., 1996; Kuhara et al., 2002; Okochi et al., 2005; Inada et al., 2006; Biron et al., 2006). The thermal sensor molecule remains uncertain, although some evidence suggests that it is SRTX-1, a GPCR specifically expressed in AFD neurons (Colosimo et al., 2004; Biron et al., 2008). Transmission electron microscopy (TEM) ultrastructural studies have shown that AFD neuron sensory endings possess ~50 small membrane projections called fingers or villi, as well as a 'rudimentary' cilium (Perkins et al., 1986). This high ratio of membrane surface area to volume presumably contributes to the sensitivity of this neuron to temperature changes as small as 0.05℃ (Clark et al., 2006). In contrast, the function of the short cilium is unknown. Tan and colleagues found that disrupting BBS proteins results in abnormal thermotaxis (Tan et al., 2007), but their actual mechanistic contribution to this behavior remains unclear.

Here, we demonstrate that ciliary proteins modulate the localization of cGMP signaling components in AFD neurons. Specifically, we show that proper localization of cGMP signaling proteins to different membrane compartments requires the MYND-domain-containing protein DAF-25, the BBSome protein BBS-8 and the transition zone network component NPHP-2. Moreover, we identify the finger membrane as a subcompartment of the ciliary structure in AFD neurons, with a newly identified membrane barrier that might act as a transport hub for signaling proteins functioning in the cilium. Interestingly, this gate contains a cellular junction marker and some components present are the same as those within the ciliary transition zone, although it lacks canonical Y-link structures. Our findings help establish the AFD neurons as a model system to study the connection between ciliary trafficking and the formation of discrete cGMP signaling compartments.

RESULTS

cGMP signaling components localize to separate compartments with different lipid compositions in AFD neurons

The GPCR SRTX-1 and guanylyl cyclases GCY-8, GCY-18 and GCY-23 – signaling proteins required for thermotaxis – have been previously found to localize to the finger-containing region proximal to the cilium found at the very tip of AFD neurons (Colosimo et al., 2004; Inada et al., 2006). However, it was unclear whether these proteins were also present in the cilium, an established sensory organelle. We therefore investigated the localization of various cGMP signaling components in relation to the cilium by co-expressing their RFP-tagged versions with ARL-13::GFP, a well-established ciliary membrane marker (ortholog of mammalian ARL13B; Cevik et al., 2010). An AFD-specific version of ARL-13::GFP localized predominantly to one single projection distal to the fingers, consistent with the ciliary location known from TEM analysis. Notably, less intense staining was also observed in the AFD fingers, but not the dendritic membrane (Fig. 1A,B). The cilium marked by ARL-13::GFP is often elongated and exhibits extra membrane at the distal end, which could be caused by the overexpression of ARL-13 as described previously (Cevik et al., 2010).

Interestingly, there was a segregation of cGMP signaling proteins into different domains. Fluorescently tagged versions of SRTX-1 and guanylyl cyclase proteins (represented here by GCY-18) with their endogenous promoter were expressed only in AFD neurons, consistent with previous reports (Colosimo et al., 2004; Inada et al., 2006). More specifically, these proteins localized exclusively to the finger membrane, but not the cilium, of AFD neurons (Fig. 1A). The CNG channel subunit TAX-4 (known as CNGA1 in mammals), however, is present in various ciliated neurons. In AFD neurons, it was found in the proximal part of the cilium, and not the fingers (Fig. 1B). This is similar to the location of the subunits TAX-2 (known as CNGB1 in mammals) and TAX-4 at the proximal region of the ciliated AWB and ASK neurons (Mukhopadhyay et al., 2008; Wojtyniak et al., 2013).

GPCR and guanylyl cyclase protein localization to the extensive membrane area of the fingers in AFD neurons might help increase its sensitivity to temperature changes. However, the advantage of having ion channels present only in the cilium is not clear. One possibility is that the lipid environment needed for ion channel function differs from that needed for thermosensation. We therefore probed the lipid composition of the AFD dendritic endings using GFP constructs carrying different lipid anchors (Zacharias et al., 2002). Two GFP constructs with saturated fatty acid chains (myristoylated plus palmitoylated, and tandemly palmitoylated) are present throughout the dendritic, finger and, possibly, ciliary membranes of the AFD neurons. In contrast, geranylgeranylated GFP, which has an unsaturated fatty acid anchor, localizes specifically to the finger membrane (supplementary material Fig. S1). This suggests a different lipid composition between the finger membrane and the rest of the membrane at the AFD dendritic end.

Downstream of CNG channels, various voltage-gated ion channels help propagate and modulate neuronal activation.

Journal of Cell Science (2014) 127, 5317–5330 doi:10.1242/jcs.157610

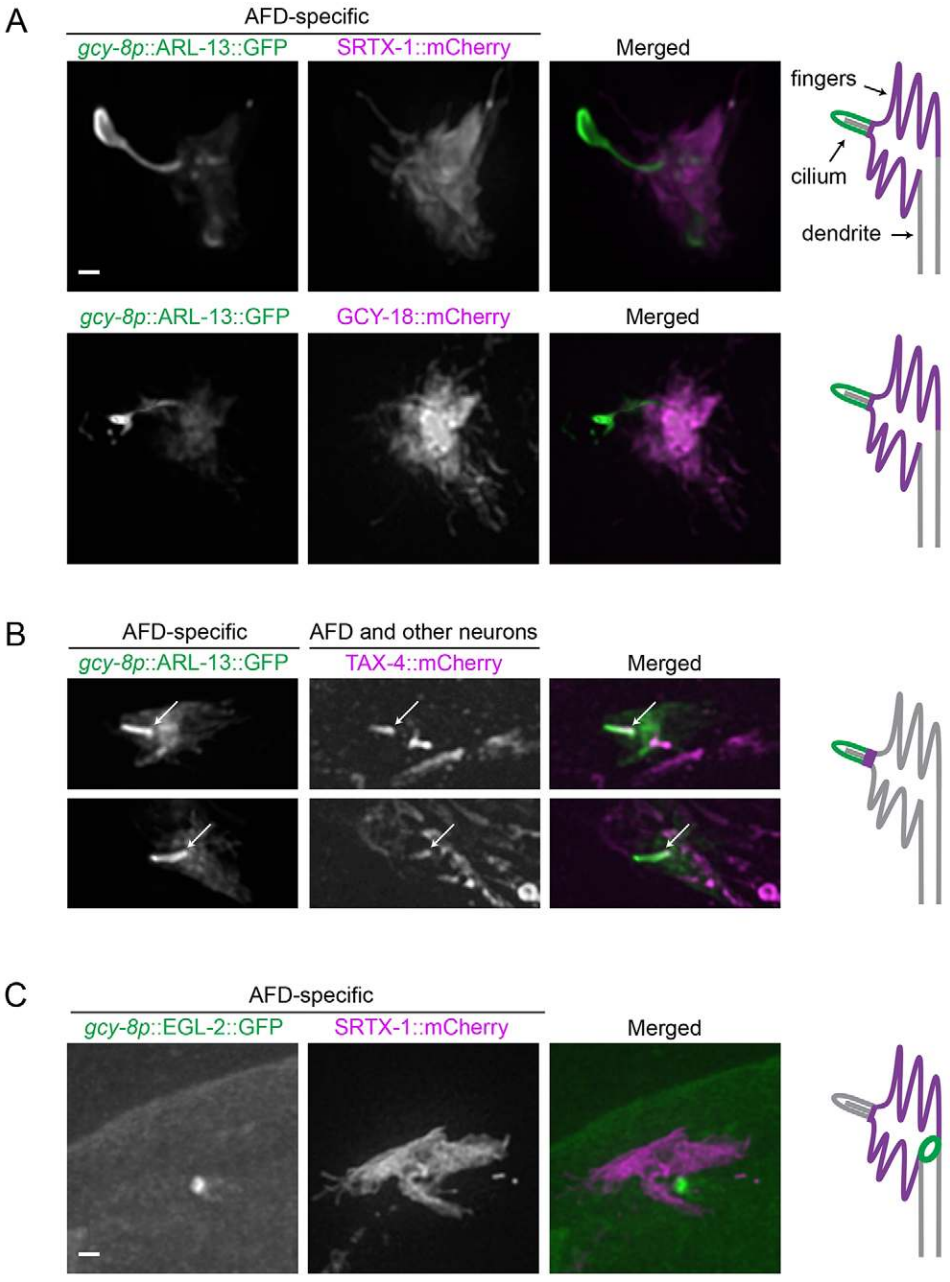

Fig. 1. cGMP signaling components are localized to two distinct compartments in AFD neurons. (A,B) Fluorescently tagged membrane proteins in the cGMP signaling pathway are coexpressed with ARL-13, a ciliary membrane marker, driven by an AFD-specific promoter (*gcy-8p*). (A) SRTX-1 and GCY-18 are AFD-specific, and present within the finger membrane but not the cilium. (B) TAX-4 is expressed in many ciliated neurons besides AFD neurons, and is localized specifically to the proximal part of the AFD cilium (arrows). Two representative images are shown for TAX-4. (C) EGL-2, an EAG K^+ channel, shows ring-like localization pattern at the base of the finger compartment in AFD neurons, as marked by SRTX-1. Schematics of the two compartments and localization of signaling components are depicted on the right of the panels (only six fingers are drawn, there are normally about 60). Scale bars: 1 μm.

EGL-2 is an ether a-go-go (EAG) K^+ channel present in *C. elegans* sensory neurons, including AFD, that influences taxis behaviors through sensory processes (Weinshenker et al., 1999). Given that EGL-2 could participate in electrical signaling downstream of a cGMP cascade, we investigated its localization in AFD neurons. Interestingly, EGL-2 was concentrated within a ring-like domain between the finger and dendritic membranes (Fig. 1C). This close proximity to the cGMP signaling compartment, just before the electrical signal propagates down the dendrite, suggests that EGL-2 might be regulated by cGMP signaling directly or indirectly and helps set the excitability of AFD neurons for optimal thermotaxis.

Localization patterns of ciliary proteins indicate that AFD fingers represent a cilium-related subcompartment

The observation that the ciliary membrane marker ARL-13 is also present on the fingers but not dendritic membrane in AFD neurons (Fig. 1A,B), even when injected at very low concentrations, suggests that the finger membrane is more similar in composition to the ciliary, rather than dendritic, membrane. To investigate the possibility that the finger compartment may be related to the cilium, we analyzed the localization of various ciliary proteins in AFD neurons. In these studies, we used fluorescently labeled SRTX-1 as the marker for the finger compartment, and observed the localization patterns of various ciliary proteins driven by an AFD neuron-specific promoter.

We first looked at XBX-1 (known as DYNC2LI1 in mammals), a dynein motor subunit of the IFT machinery shown to be present at the base and along the length of the axoneme of canonical cilia in other neurons (Schafer et al., 2003). In AFD neurons, XBX-1 concentrated at the ciliary base and along the axoneme (Fig. 2A), as expected given that microtubule tracks can be observed within

Journal of Cell Science (2014) 127, 5317–5330 doi:10.1242/jcs.157610

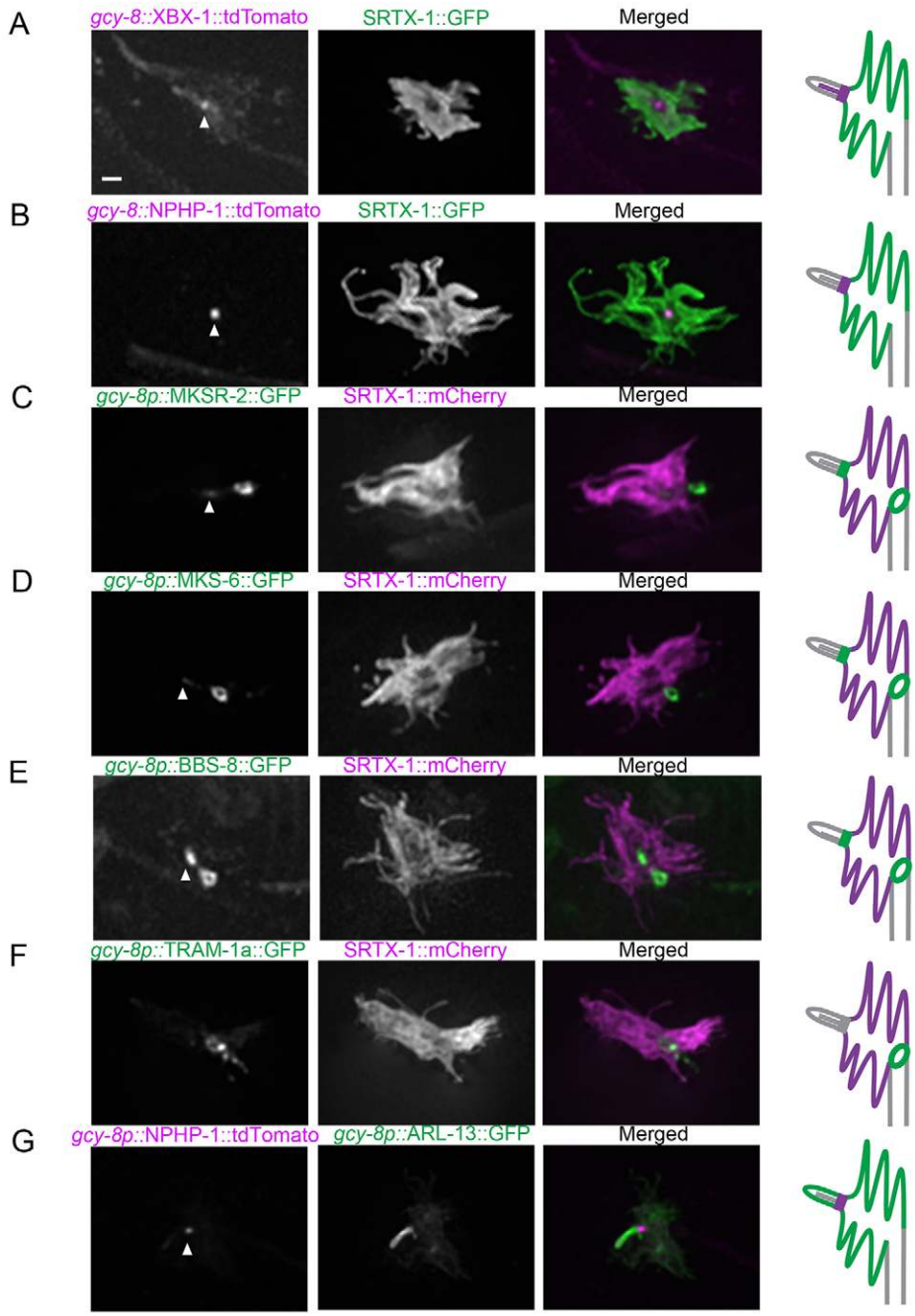

Fig. 2. Localization of ciliary and dendritic protein markers uncovers the AFD finger compartment as a cilium-related subcompartment. Fluorescently tagged ciliary proteins were produced specifically in the AFD neurons and co-expressed with SRTX-1, a marker of the AFD finger membrane. The IFT-dynein subunit XBX-1 (A) and transition zone protein NPHP-1 (B) are enriched at the base of the cilium. The transition zone proteins MKSR-2 (C) and MKS-6 (D) are localized at the base of the cilium and are also present as ring structures between the finger and dendritic membranes. (E) BBS-8 is also localized in the cilium and at the ring structure. (F) TRAM-1a, which is normally found at the dendritic tips but not inside cilia, is present at the ring outside of the finger compartment in AFD neurons. (G) Co-expression with ARL-13 confirmed that NPHP-1 signal is at the base of the cilium. Arrowheads indicate the base of the cilium. Scale bar: 1 μm.

the short cilium of AFD neurons in TEM images (Perkins et al., 1986).

Next, we looked at several members of the transition zone protein network (Williams et al., 2011). As expected, NPHP-1 (known as NPHP1 in mammals) is enriched near the ciliary base in AFD neurons (Fig. 2B,G), consistent with the presence of Y-links in this region (Perkins et al., 1986). However, to our surprise, besides the ciliary base, the transition zone network proteins MKSR-2 (known as B9D2 in mammals) and MKS-6 (known as MKS6 and CC2D2A in mammals) also displayed a second, more prominent localization, as a ring structure between the distal end of the dendrite and finger compartment (Fig. 2C,D). That MKSR-2 and MKS-6 show a somewhat different localization pattern than NPHP-1 might reflect their involvement in two related, yet distinct transition zone protein modules (MKS and NPHP modules, respectively) (Williams et al., 2011; Sang et al., 2011).

In all ciliated sensory neurons examined to date, BBS-8 (the BBS8 ortholog) is specifically found at the basal body, where IFT particles dock, and along the ciliary axoneme, in association with moving IFT particles (Blacque et al., 2004; Williams et al., 2011). Surprisingly, BBS-8 was also found at two different locations in AFD neurons: concentrated at the ciliary base (as expected) and at the ring structure (Fig. 2E). To further support the hypothesis that the finger membrane represents a cilium-related subcompartment, we studied the localization in AFD neurons of isoform a of TRAM-1 (TRAM-1a; known as TRAM1 in mammals), a membrane protein normally found outside cilia,

Journal of Cell Science (2014) 127, 5317–5330 doi:10.1242/jcs.157610

near the basal body (Bae et al., 2006; Williams et al., 2011). We observed TRAM-1a predominantly at the ring structure just outside of the finger area in AFD neurons (Fig. 2F), suggesting that this structure might serve as a barrier between the finger and dendritic membranes in AFD neurons. Taken together, these data suggest that the AFD fingers represent a cilium-related subcompartment.

The cilium develops before the finger compartment

Having established the spatial relationship between the two presumptive signaling compartments, we were interested to know whether the cilium or finger compartment forms first. The temporal relationship between these two compartments could potentially give us insight into how the cGMP signaling cascade is established in AFD neurons. To investigate the development of these two compartments, the appearance of fluorescent SRTX-1 (a finger membrane marker), ARL-13 (a ciliary membrane marker) and MKS-6 (a transition zone marker) at the site of ciliogenesis were followed in AFD neurons during embryogenesis. ARL-13 appeared early at the site of the developing cilium at the 2-fold embryonic stage (Fig. 3A), consistent with the onset of ciliogenesis (Sulston et al., 1983; Swoboda et al., 2000). At the early 3-fold stage, the MKS-6 signal starts to be seen at the ciliary site as one distinct punctum, suggesting the formation of a transition zone, the first ciliary structure to form as proposed by Williams et al., 2011 (Fig. 3B). Our observation that ARL-13 can be seen at the ciliary site earlier than MKS-6 is consistent with the recent finding by Ruppersburg and Hartzell (Ruppersburg and Hartzell, 2014) that during ciliogenesis, the ciliary membrane can be defined before the migration of the centriole to the apical membrane, and therefore preceding transition zone formation. When SRTX-1 becomes

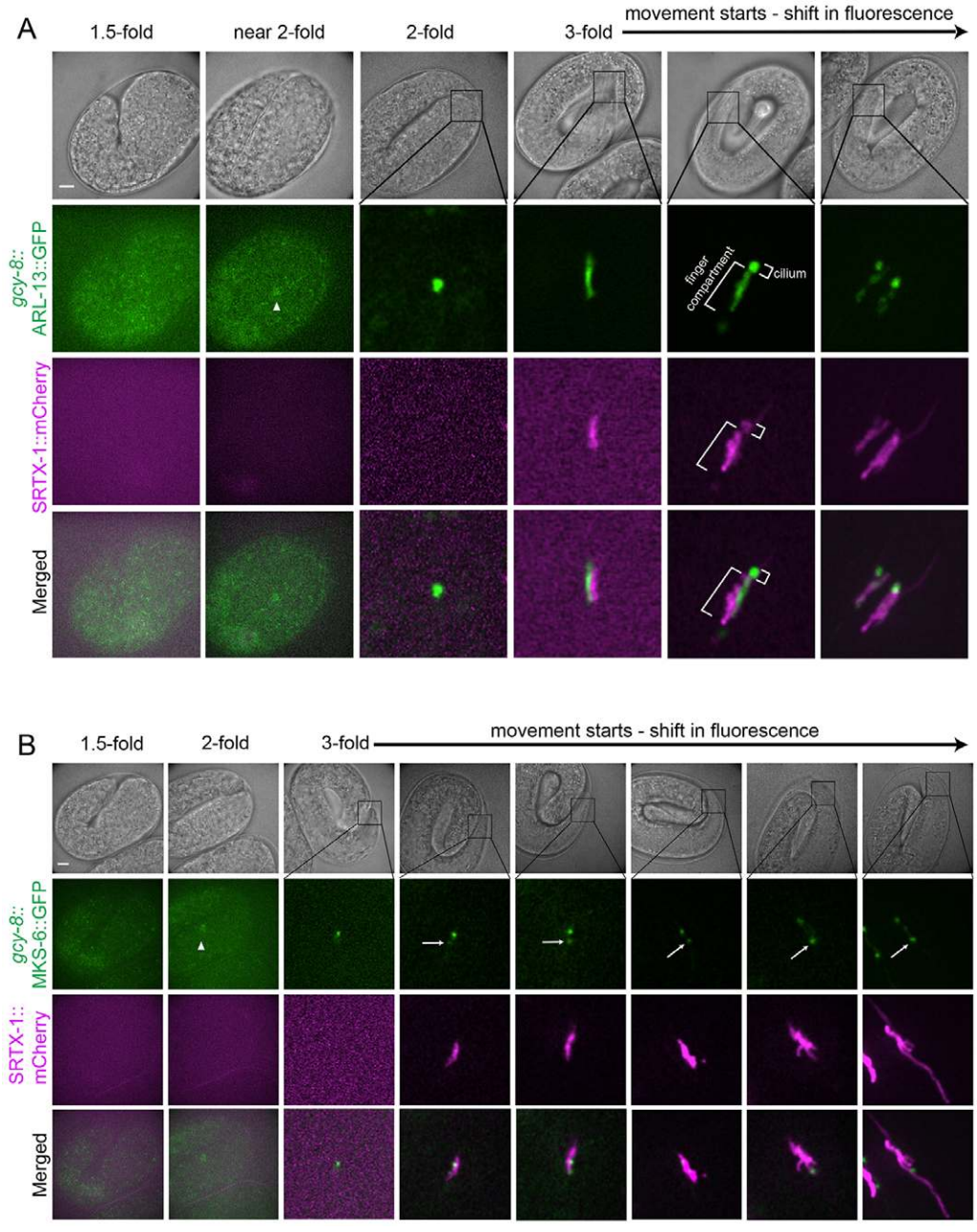

Fig. 3. Development of the cilium precedes finger formation. The development of the ciliary and finger compartments in AFD neurons are shown at various stages during embryogenesis. Non-overlapping signals at the 3-fold stage are caused by slight movement of the embryos, which could not be completely eliminated without affecting their development during the experimental time period. (A) Ciliary membrane (marked by ARL-13) appears before the fingers (marked by SRTX-1) are formed. (B) The transition zone protein MKS-6 appears first at the base of the cilium, and then at a more posterior second location (arrows), as the finger compartment (marked by SRTX-1) develops. Arrowheads indicate AFD cell bodies. Scale bars: 5 µm.

Journal of Cell Science (2014) 127, 5317–5330 doi:10.1242/jcs.157610

visible later at the 3-fold stage, its signal overlapped with ARL-13 in a rod shape, and their signals gradually separate, albeit not completely, before any fingers are detectable (Fig. 3A). In the meantime, a second MKS-6 signal split away from the anterior and original transition zone, and these two signals moved away from each other as the finger compartment grew (Fig. 3B). Our data are therefore the first to describe, using endogenous markers, a pre-finger compartment. The fingers were formed last, at the late 3-fold stage (Fig. 3B). Our observations suggest that the cilium forms before the finger compartment, and further support the finding that the two compartments are related, initially arising from the same progenitor membrane.

The ring structure is not a typical transition zone

Because of its potential role in compartmentalizing and trafficking proteins in the AFD dendritic end, we further investigated the ciliary-protein-containing ring structure present around the base of the finger compartment. We found that this structure, when marked by MKS-6, persists in worms lacking DAF-19, the RFX transcription factor required for ciliogenesis in *C. elegans* (Swoboda et al., 2000) and which plays a conserved role in vertebrate ciliogenesis (Choksi et al., 2014). Furthermore, the MKS-6 signal was retained in the absence of MKS-5 (known as MKS5 and RPGRIP1L in mammals), a core transition zone protein required for proper localization of all transition zone proteins tested (Huang et al., 2011; Williams et al., 2011) (Fig. 4A). These data suggest that the localization of MKS-6, an established transition zone protein containing a lipid-binding C2 domain, to the ring structure is likely to be independent of the ciliary machinery.

The ring structure is not a canonical transition zone because earlier TEM revealed no structures reminiscent of transition zone Y-links between the finger and dendritic membranes (Perkins et al., 1986). However, it could still act as a membrane barrier,

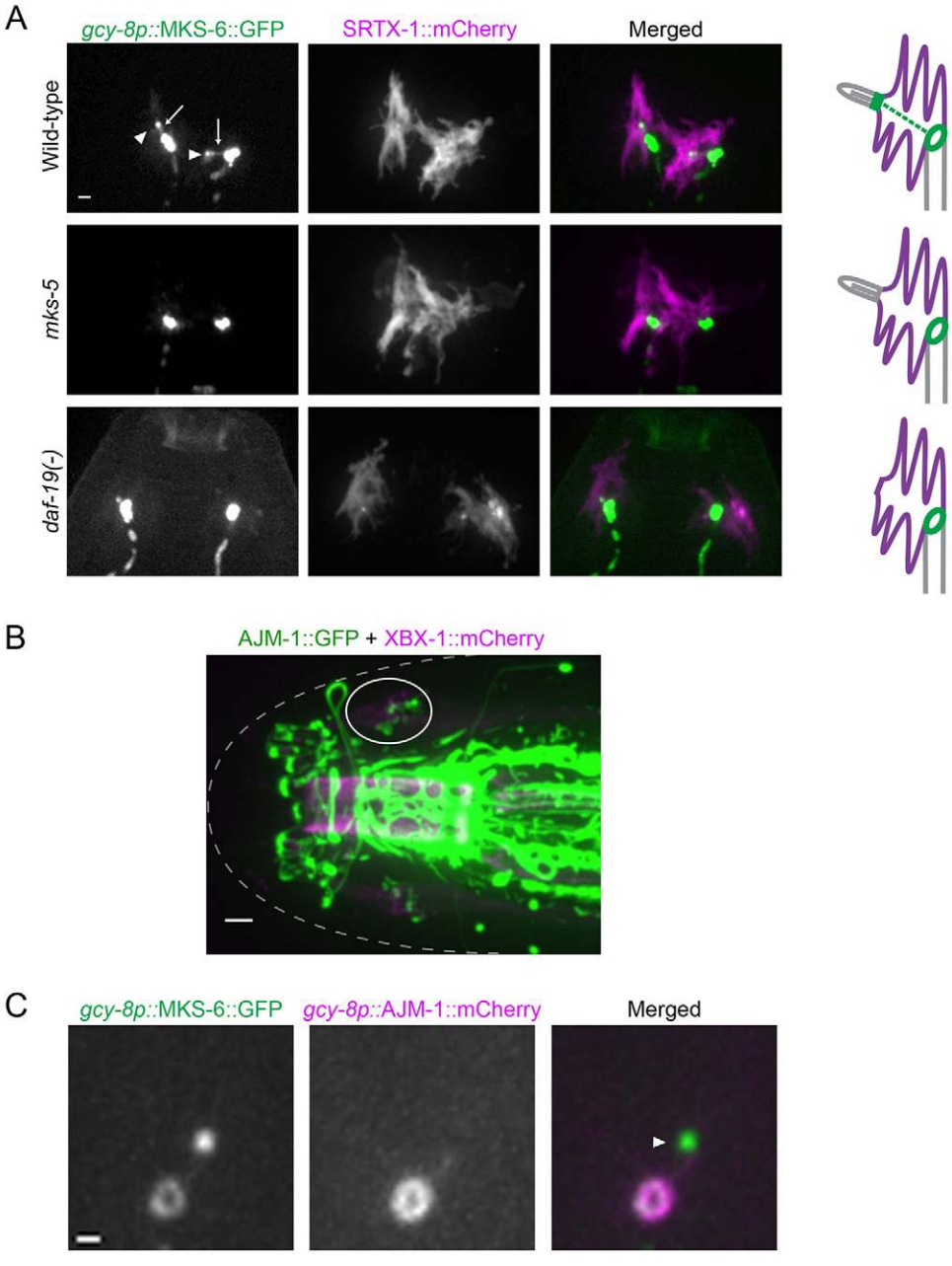

Fig. 4. An apical junction separates the finger compartment from the dendritic membrane. (A) The ring-like structure is still present in mutants lacking the ciliary transcription factor DAF-19 or the essential transition zone protein MKS-5. Two neurons are shown for each worm. GFP signals are overexposed to highlight the complete absence of the canonical transition zone in the mutants (arrowheads in wild-type). Overexposure also shows a filamentous structure in wild-type worms decorated with MKS-6 that could be IFs (arrows). Scale bar: 1 μm. (B) In the head, apical junctions (marked by AJM-1) are seen as ring-like structures at the base of cilia (marked by XBX-1) in the bilateral amphid channels (one side is circled). Scale bar: 2 μm. (C) AJM-1 is colocalized with MKS-6 at the ring in AFD neurons. Note the absence of AJM-1 at the canonical transition zone (arrowhead). Scale bar: 0.5 μm.

Journal of Cell Science

Journal of Cell Science (2014) 127, 5317–5330 doi:10.1242/jcs.157610

similar to a canonical transition zone. Moreover, dark material at the membrane is seen around this area, typical of apical ('belt') junctions, special types of adherens junctions in *C. elegans*. Indeed, we find that AJM-1, an apical junction marker (Köppen et al., 2001), also showed ring-like patterns around the base of amphid cilia (Fig. 4B). In AFD neurons, AJM-1 co-localizes with MKS-6 at the ring structure, but is absent from the canonical transition zone (Fig. 4C). Interestingly, mammalian NPHP module transition zone proteins have been found at cell–cell junctions in previous studies (NPHP1, NPHP4; Donaldson et al., 2000; Mollet et al., 2005).

Supporting the ciliary gating function of transition zone proteins, Williams et al. (Williams et al., 2011) have shown that TRAM-1a leaks into the cilia of transition zone mutants. We tested whether TRAM-1a penetrated the finger compartment in transition zone mutants, but it displayed normal localization; in addition, no noticeable leakage of signaling proteins from the finger compartment was observed (data not shown). Additional studies will therefore be needed to assess the potential role of transition zone proteins at the ring structure.

Actin and intermediate filament are potential trafficking routes of ciliary proteins

How are ciliary proteins destined to the cilium transported from the apical junction, across the finger compartment, and to the cilium in AFD neurons? We hypothesized that microtubules might form the cytoskeletal tracks needed for this purpose. To address this, we carried out electron tomography of the AFD dendritic end in combination with high-pressure freezing (Fig. 5). This sample preparation improves on the previous chemical fixation method used by Perkins et al. (Perkins et al., 1986); it can avoid artifacts such as membrane swelling, and preserve delicate structures such as microfilaments and small vesicles. Doroquez et al., (2014) recently produced a tomogram of the whole AFD dendritic ending that is consistent with our results presented below, albeit with fewer details of the inside compartment (Doroquez et al., 2014).

To our surprise, no microtubule structures within the finger compartment were visible, but instead, intermediate filaments (IFs) were seen running in the middle of the compartment, with occasional vesicles seen nearby (Fig. 5). Incidentally, upon increasing expression levels (or image exposure) of MKS-6::GFP, we observed signals along a filamentous structure that could be the same as the IFs seen by electron microscopy (Fig. 4A). Electron tomography also showed actin filaments in the finger compartment, supporting the extensive membranous fingers (Fig. 5A). This finding establishes the fingers as true microvilli, which has been speculated previously but not demonstrated (Perkins et al., 1986). This component of the cytoskeleton could also be involved in trafficking, or anchoring signaling proteins such as guanylyl cyclases and SRTX-1 within the finger membrane, as seen for Na^+ channels at the node of Ranvier (Kaplan et al., 2001).

Normal localization of guanylyl cyclases requires DAF-25 and BBS proteins

Given the importance of ciliary proteins in cellular signaling, and their close association with cGMP signaling proteins at the dendritic end of AFD neurons, we wondered whether different ciliary proteins might modulate the localization of cGMP signaling components in the finger and ciliary compartments. We first examined the *daf-25* mutant, which lacks the membrane guanylyl cyclases DAF-11 and GCY-12 in other cilia (Jensen et al., 2010; Fujiwara et al., 2010). In *daf-25* mutant [*daf-25(−)*] worms, the three AFD-specific guanylyl cyclases (GCY-8, GCY-18 and GCY-23) were completely absent from the AFD fingers, but instead were found along the dendrite in some worms (Fig. 6A). Using SRTX-1 as a marker, we also observed various defects in the finger structure of the *daf-25* mutant: 35% lacked fingers, 55% had stunted fingers, and 10% displayed long, protruding fingers (Fig. 6B). Consistent with these observations, our TEM data revealed that *daf-25* AFD neurons had few, if any, fingers, which were also disorganized, in contrast to wild-type worms, where numerous fingers run parallel to each other (supplementary material Fig. S2A). Other cilia in the amphid neurons of *daf-25* worms are superficially normal, similar to those described by Jensen et al., 2010. Taken together, our data suggest that DAF-25 is essential for the trafficking of guanylyl cyclases and morphogenesis of a specialized sensory compartment.

Given that guanylyl cyclases were observed along AFD dendrites but not fingers of *daf-25* mutants, we assessed the integrity of the ring structure separating the two membranes in the mutants. Remarkably, MKS-6 was markedly reduced or completely absent from the ring in the mutants, whereas its signal was increased along the filamentous structure between the ring and canonical transition zone (Fig. 6C). Although apical junctions near amphid cilia of *daf-25* worms appeared intact (supplementary material Fig. S2B), our data suggest that the integrity of this barrier is compromised, resulting in a transition zone protein (MKS-6) leaking through the docking zone while others (guanylyl cyclases) are prevented from entering the finger compartment.

We also examined mutations in BBS-8, given its presence at both locations relevant to cGMP signaling proteins – the cilium, which harbors the cGMP-gated channel TAX-4, and ring structure at the entrance to the finger compartment, where SRTX-1 and guanylyl cyclases are found (Fig. 1A,B; Fig. 2E). Although *bbs-8* mutants showed normal localization of many different cGMP signaling components tested (SRTX-1, TAX-2, TAX-4, TTX-4 and TAX-6), they showed mislocalization of the guanylyl cyclase proteins (26%, 46% and 30% of AFD neurons were abnormal for GCY-8, GCY-18 and GCY-23, respectively) (Fig. 6D, supplementary material Fig. S3). Whereas wild-type worms showed guanylyl cyclase localization only in the finger compartment, *bbs-8* worms also had guanylyl cyclases along the dendrite, and variable, strong accumulation in the fingers. Importantly, we confirmed this phenotype in *bbs-7* mutants (Fig. 6E), demonstrating that the overall function of the BBSome is important for guanylyl cyclase localization in AFD neurons. Notably, this phenotype was not observed upon disruption of OSM-5 and CHE-11 (known as IFT88 and IFT140, respectively, in mammals), which impair anterograde and retrograde IFT, respectively (Fig. 6E). Given that BBS proteins are normally associated with the IFT machinery, our findings suggest that BBS proteins might unexpectedly act in an IFT-independent manner to facilitate guanylyl cyclase trafficking to and/or from the finger compartment.

Correct localization of the TAX-4 channel requires DAF-19 and NPHP-2

The cGMP-gated channel subunit TAX-4 localized within the proximal part of the AFD cilium (Fig. 1B), yet appeared to be unaffected by the disruption of BBS-8 or DAF-25 (supplementary material Fig. S3; Jensen et al., 2010). We wondered whether other

Journal of Cell Science (2014) 127, 5317–5330 doi:10.1242/jcs.157610

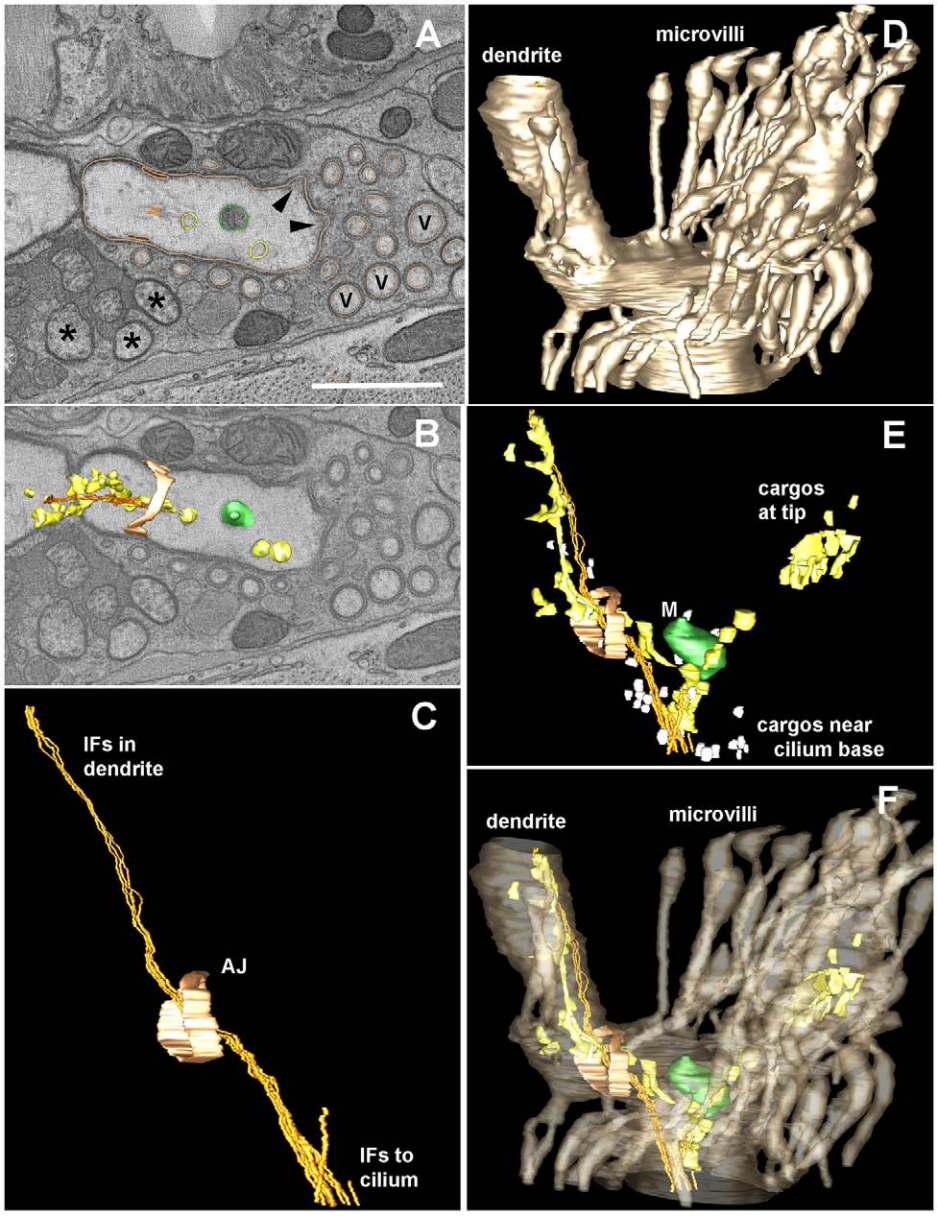

Fig. 5. Electron tomography reveals the structure of the AFD dendritic ending. An electron tomogram was produced from thick serial sections for a distal portion of the AFD dendrite, in order to highlight details of the microvilli, the apical junction (AJ, pale orange) to the surrounding amphid sheath cell, and the various contents within the finger compartment, which lie along a cluster of IFs that span from the distal dendrite to the base of the cilium. (A) Orthoslice through a portion of the tomogram showing a variety of objects that have been modeled using IMOD to trace their contours, including a mitochondrion (green) and larger vesicles (beige) that might represent smooth ER. Several closely spaced IFs (gold) run as a tight bundle, with these other small objects lying close by. No microtubules were identified within this region. Several amphid channel cilia (asterisks) and several additional microvilli (V) that were not traced are indicated. Arrowheads indicate the base of two traced microvilli; their cytoplasm is locally more electron dense, representing diffuse actin just beneath the plasma membrane. The outline of traced microvilli is shown in the same color as the AFD plasma membrane (beige). Scale bar: 1 μm. (B) A nearby orthoslice shows three-dimensional features of several modeled objects to better display how they fit within the distal dendrite. (C) Side view of modeled region highlights the extension of the IF bundle from inside the distal dendrite, running past the apical junction to enter the finger compartment. This IF bundle continues anteriorward, outside of the tomogram to reach the base of the cilium (not shown), further anterior to the tomogram. (D) Lateral view of the modeled region highlighting the plasma membrane of AFD (in beige), including the distal dendrite and part of the finger compartment. (E) Same model view as C and D, showing the multiple cargoes that lie along the IF bundle. Close to the base of the cilium, many small vesicles (white) cluster near the IF bundle. Smooth ER clusters along the IF bundle both inside the dendrite and within the finger compartment. (F) Same view as panels C, D, E, highlighting the clustering of cargos inside the finger compartment, but with no cargos entering into the surrounding microvilli.

ciliary proteins were required for its proper localization. We first tested DAF-19, which is essential for ciliary gene expression and hence formation of all cilia in *C. elegans* (Swoboda et al., 2000). Compared to wild-type worms, where TAX-4 localizes near the ciliary base and sometimes accumulates at the ring structure in AFD neurons, in *daf-19* animals TAX-4 concentrated within the finger compartment, possibly along the filamentous structure between the cilium and ring structure (Fig. 7A). This suggests that the filamentous structure might normally help traffic TAX-4 from the AFD dendrite to the cilium.

Journal of Cell Science (2014) 127, 5317–5330 doi:10.1242/jcs.157610

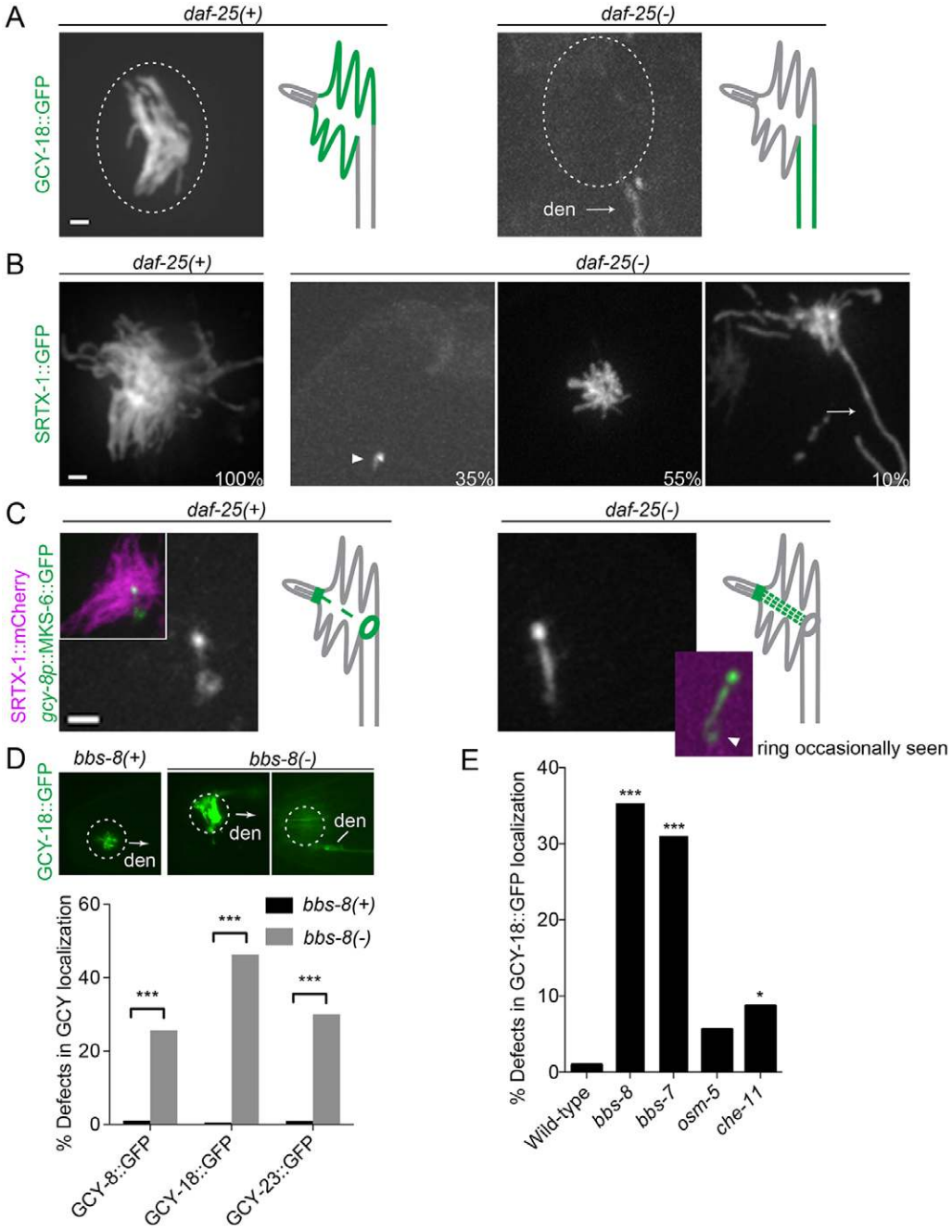

Fig. 6. The *daf-25* and *bbs-8* mutants show defects in the localization of guanylyl cyclases. (A) Localization of guanylyl cyclases in wild-type and *daf-25(-)* worms. Guanylyl cyclases, represented here by GCY-18, are absent from AFD fingers of the *daf-25* mutant, and are seen along the dendrite (den) instead. Dotted ovals indicate the position of the finger compartment. (B) *daf-25(-)* worms show defects in finger formation. The numbers are the percentages of worms with each phenotype (n=100). The arrowhead indicates a complete absence of fingers, and the arrow points to an extra-long finger. (C) The transition zone protein MKS-6 displays an altered localization in *daf-25* worms, as it appears stronger at the filamentous structure connecting the cilium and the ring structure (arrowhead indicates the signal occasionally seen in the ring structure in the mutant). Scale bars: 1 μm. (D) Localization of a representative guanylyl cyclase (GCY-18::GFP) in wild-type and *bbs-8* worms. GCY-18 is localized specifically in the finger compartment of wild-type AFD neurons, but accumulates in the fingers and along the dendrite of the *bbs-8* mutant. In the image on the right for *bbs-8(-)*, the plane was focused on the dendrite to highlight the accumulation there, this neuron still has GFP signal in the finger compartment. Arrows indicate the direction of the dendrite when it is not visible. The graph shows the percentage of AFD neurons with defective localization of each guanylyl cyclase (n>100). (E) Mislocalization of GCY-18 is a prominent phenotype in *bbs* mutants (*bbs-7*, *bbs-8*) but not other mutants that affect IFT (*osm-5* and *che-11*). The bar graph shows the percentage of AFD neurons with defective GCY-18 localization (n>100). *P<0.05; ***P<0.001 (compared with wild-type, χ^2 test).

In amphid cilia, TAX-4 localizes just distal to the transition zone, as with the inversin ('inv') compartment in mammalian cells (Shiba et al., 2009). There, inversin (INVS or NPHP2) helps anchor two proteins, NPHP3 and NEK8, which together might form a functional complex (Shiba et al., 2010). We therefore questioned whether the *C. elegans* inversin ortholog NPHP-2, which is localized to the 'inversin compartment' (Warburton-Pitt et al., 2012), is required for maintaining TAX-4 to this region. We confirmed that fluorescent-tagged TAX-4 colocalized with NPHP-2 in the proximal segment of amphid cilia, distal to the transition zone (marked by MKSR-2) and the basal body (marked by XBX-1) (Fig. 7B). Interestingly, in *nphp-2* mutants, TAX-4 failed to localize tightly to this region, being partially delocalized to the distal ciliary region, and no longer appearing to be membrane associated (Fig. 7C). Given that the cilium of AFD neurons is short, and the signal of TAX-4::GFP in these neurons is even smaller, we could not conclusively test whether TAX-4 was mislocalized in AFD neuron cilia in *nphp-2* mutants. However, *nphp-2* mutants had thermotaxis defects suggestive of abrogated TAX-4 function (see below).

Ciliary proteins are required for thermotaxis

Given the mislocalization of guanylyl cyclases (GCY-8, GCY-18 and GCY-23) in *daf-25* and *bbs* mutants, and of TAX-4 in the *daf-19* and *nphp-2* mutants (Figs 6, 7), we expected that these mutants would exhibit thermotaxis defects. Only *bbs* mutants have been previously tested, with data suggesting thermosensation and/or thermotaxis defects (Tan et al., 2007). Indeed, our findings indicate thermotaxis defects in *daf-25*, *bbs-8*, *daf-19*, and *nphp-2* mutants (supplementary material Fig. S4A). However, we noted that in the

Journal of Cell Science (2014) 127, 5317–5330 doi:10.1242/jcs.157610

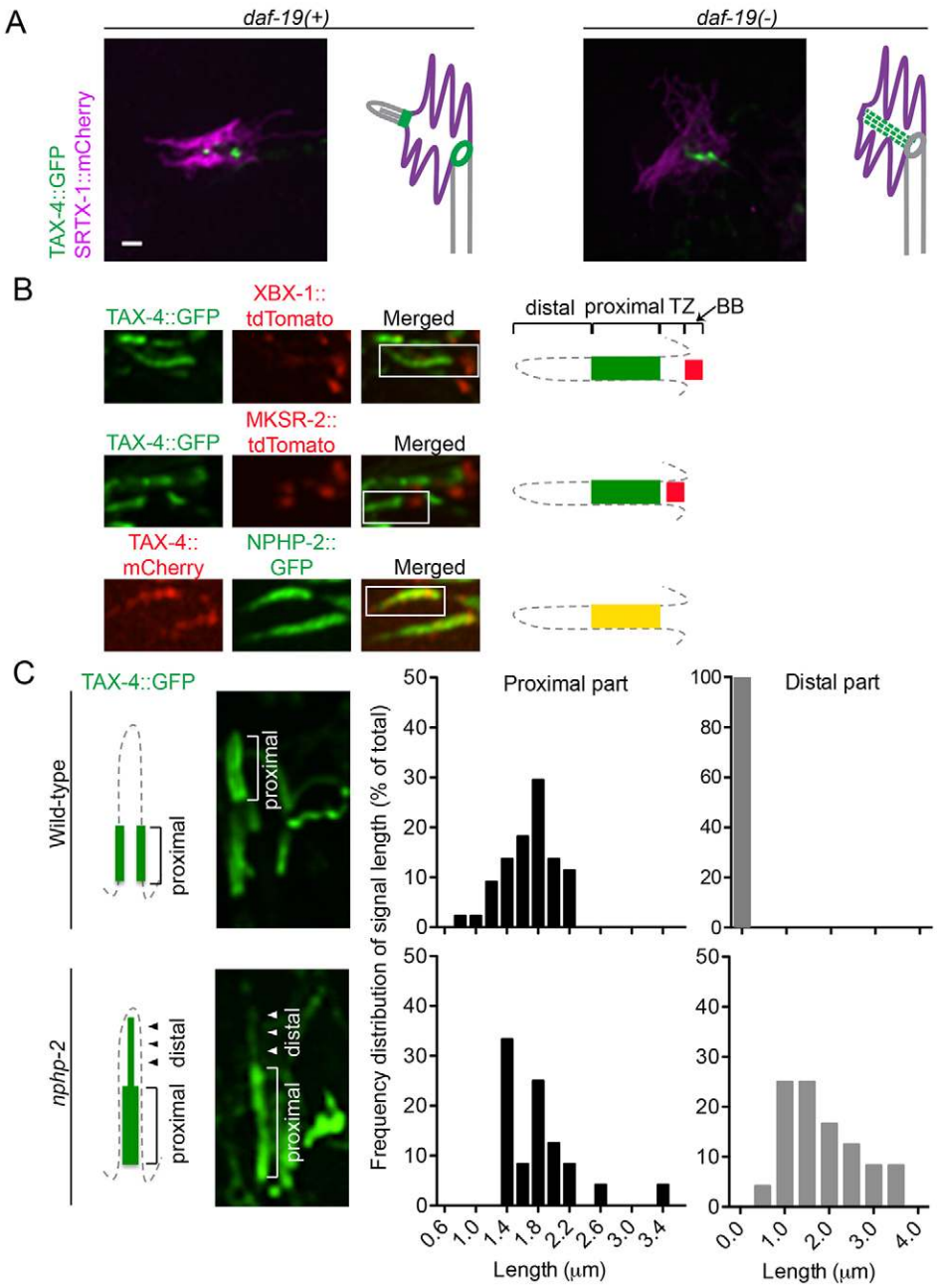

Fig. 7. The *daf-19* and *nphp-2* mutants show defects in the localization of TAX-4. (A) TAX-4 is mislocalized in the *daf-19* mutant. Instead of its wild-type localization at the ciliary base, TAX-4 in the *daf-19* mutant is seen in the finger compartment, probably along the IFs. (B) TAX-4 localizes to the inversin compartment of the cilium. In amphid channel cilia, TAX-4 colocalizes with NPHP-2 in the proximal part of the cilium, above the transition zone (TZ, marked by MKSR-2) and the basal body (BB, marked by XBX-1). (C) TAX-4 is mislocalized in amphid cilia of the *nphp-2* mutant. Wild-type cilia display discrete localization of TAX-4 at the proximal and not in the distal part of the cilia, whereas *nphp-2* cilia show GFP signal leaking into the distal part of cilia. The histograms show the frequency distribution of the signal length at proximal and distal parts in cilia of wild-type (n=44) and *nphp-2* (n=24) worms. Scale bars: 1 μm.

absence of a temperature gradient, *bbs-8*, *daf-19* and *daf-25* mutants showed reduced 'spontaneous' movement both on and off food (supplementary material Fig. S4B,C), even though their overall locomotion appeared normal when prodded with a pick. Such an exploratory phenotype has been reported for other ciliary mutants (Fujiwara et al., 2002; Gray et al., 2005), and the movement behavior is thought to be mediated by various ciliated neurons, including AFD (Gray et al., 2005; Mok et al., 2011). In contrast, the *nphp-2* mutant does not exhibit an obvious locomotory defect (supplementary material Fig. S4B,C), so its thermotaxis phenotype is likely caused by a temperature-sensing defect. Our data suggest that mutations in ciliary genes can cause thermotaxis defects, but further experiments will be needed to study how the role of ciliary proteins in cGMP signaling in AFD neurons might contribute to this phenotype.

DISCUSSION

To ensure optimal transmission of extracellular signals, signaling proteins are spatially arranged into domains where different modulator proteins, and possibly lipid environments, can efficiently regulate signal strength. This has led to the evolution of signaling centers, including cilia. In this study, we have started to unravel how ciliary proteins help establish two subcompartments that harbor different cGMP signaling components required for thermosensation in *C. elegans* AFD neurons.

Identification of a new cilium-related subcompartment bounded by transition zone proteins

Our studies suggest that the dendritic end of AFD neurons is a bipartite signaling compartment, harboring a bona fide cilium and a 'finger compartment' containing cGMP signaling proteins. This

Journal of Cell Science (2014) 127, 5317–5330 doi:10.1242/jcs.157610

is supported by the localization of ciliary proteins to both subcompartments where cGMP signaling proteins are found (Figs 1, 2), the shared developmental process of the two subcompartments (Fig. 3), and the requirement of ciliary proteins for proper protein localization to both subcompartments (Figs 6, 7). The presence of a ring-like barrier and trafficking hub between the fingers and dendrite, where ciliary proteins are found (Fig. 2), also supports the hypothesis that the fingers represent a subcompartment of the ciliary membrane in the AFD neurons. Owing to its protein composition (i.e. the presence of ARL-13 and signaling proteins and lack of TRAM-1a), and the localization pattern of guanylyl cyclases in the *daf-25* mutant, the finger compartment appears to be different from the recently described periciliary membrane compartment (PCMC) adjoining other *C. elegans* cilia (Kaplan et al., 2012). The presence of BBS, IFT and transition zone proteins in the distal end of the AFD neuron provides further evidence that this region is a canonical cilium with a transition zone and axoneme, confirming previous TEM analyses (Perkins et al., 1986). On the basis of our findings, we conclude that AFD neurons have a bipartite signaling compartment, consisting of a cilium and a finger subcompartment (Fig. 8A).

Our data also showed that in AFD neurons, signaling proteins are segregated into different ciliary membrane domains. This is similar to that found in the mammalian olfactory cilia (Menco, 1997) and the outer segment of mammalian photoreceptors (Insinna and Besharse, 2008). Interestingly, there seems to be a difference in the lipid composition of the two membrane domains, with the finger membrane lipid being less saturated and containing the putative GPCR thermosensor SRTX-1 and the guanylyl cyclases. The outer segment of photoreceptors is also rich in unsaturated lipids, which is important for rhodopsin

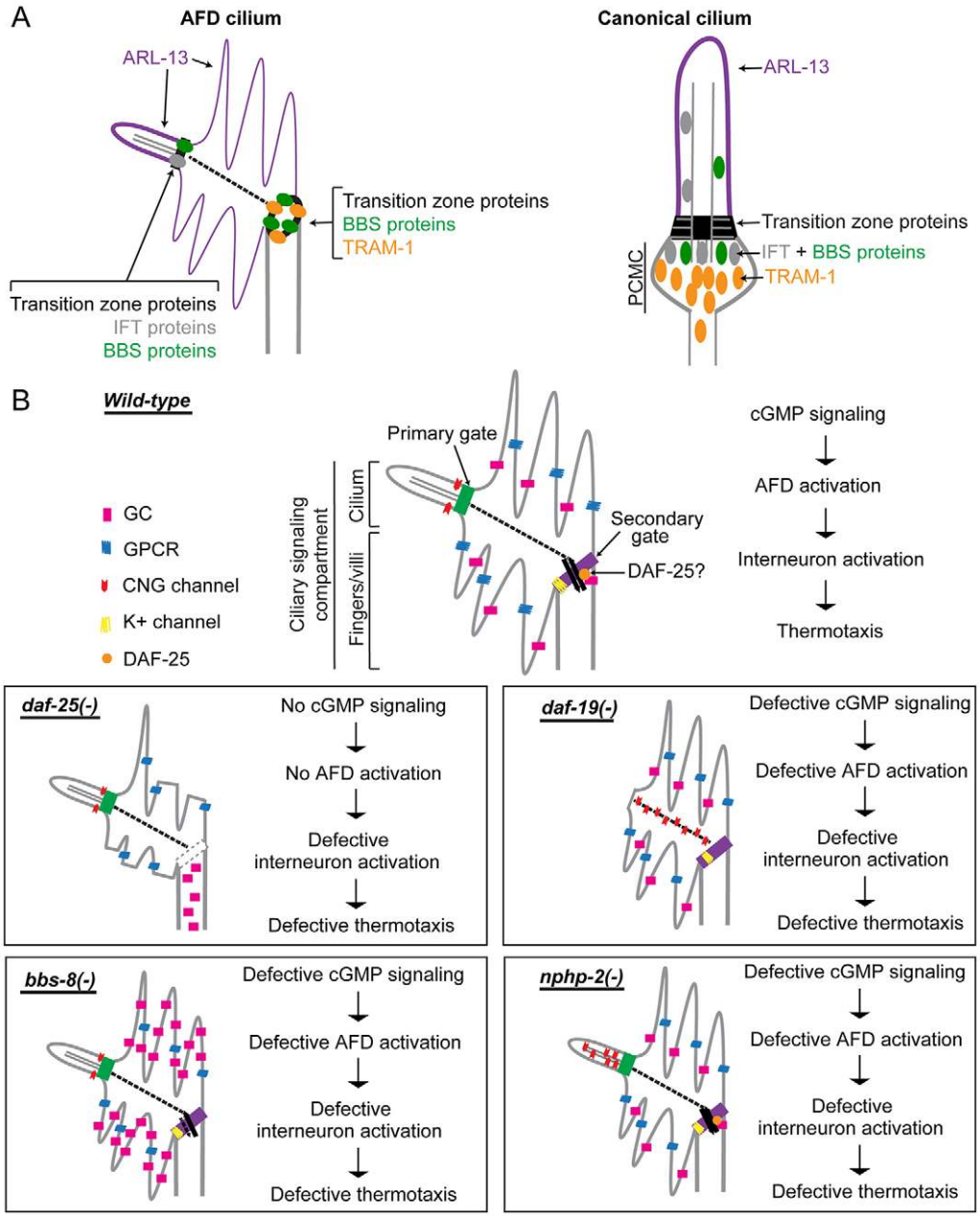

Fig. 8. Working model of cGMP signaling compartmentalization by ciliary and other proteins at AFD sensory endings. (A) In AFD neurons, ciliary proteins are present in the cilium proper and also found at the base of the finger compartment, establishing it as a cilium-related subcompartment distinct from the periciliary membrane compartment (PCMC) found in other cilia. (B) Summary of signaling compartments in the AFD cilium of wild-type and ciliary mutant worms. DAF-25 might function at the ring structure to regulate the trafficking of signaling proteins into the finger compartment. In the *daf-25* mutant, the integrity of this gate and of the fingers is compromised, and guanylyl cyclases (GC) are no longer found in the fingers, so this mutant is expected to have abrogated cGMP signaling. In the *bbs-8* mutant, accumulated guanylyl cyclases in the finger compartment could result in a high basal level of cGMP, interfering with thermotransduction. In the *nphp-2* mutant, the discrete CNG channel localization is disrupted, which could result in aberrant ion influx and defective neuronal activation. In the *daf-19* mutant, the CNG channel is present in the non-permissive membrane environment, or becomes fixed or more abundant along the IFs, and is therefore rendered non-functional. All four mutants are predicted to have altered AFD function and are therefore defective in thermotaxis.

Journal of Cell Science (2014) 127, 5317–5330 doi:10.1242/jcs.157610

function in phototransduction (Poo and Cone, 1974; Aveldaño and Bazán, 1983; Boesze-Battaglia and Schimmel, 1997). This high-fluidity lipid composition, however, might be incompatible with CNG channel function. The functions of ciliary channels are known to require a membrane rich in sphingolipids, which are saturated fatty acids (Forte et al., 1981), and lipid bilayer composition is known to substantially affect the functions of various ion channels (Schmidt et al., 2006; daCosta and Baenziger, 2009). Therefore, one function of ciliary subcompartments might be to provide appropriate lipid environment for different signaling proteins.

We also identified what might be a new type of membrane diffusion barrier between the finger and dendritic membranes, which harbors BBS and transition zone proteins that are normally found at the base of cilia (Fig. 2). Unlike in the canonical transition zone, it lacks Y-links and does not require MKS-5 to anchor the transition zone proteins. The phenotypes of *daf-25* and *bbs-8* mutants suggest that this putative barrier prevents mixing of membrane proteins, and that entry and exit of proteins through this gate is regulated (Fig. 6). The barrier also contains the apical junction marker AJM-1 (Fig. 4), providing another example of transition zone proteins present in both cilia and adherens junctions (Donaldson et al., 2000; Mollet et al., 2005), and suggesting a similarity in the function of the transition zone and adherens junction. We hypothesize that in AFD neurons, proteins are docked at the apical junction, and either function there and/or go on to be transported to the cilium.

How ciliary proteins are transported from the ring structure across the microtubule-free finger compartment into the cilium remains unclear, but our work reveals that IFs might contribute (Fig. 5). Although no motor proteins are known to move along IFs, these cytoskeletal tracks have been shown to interact with membrane-bound organelles (Styers et al., 2005), and play an important role in directional mobility of vesicles in astrocytes, independent of their interaction with microtubules (Potokar et al., 2007). The role of IFs in the finger compartment could be to restrict diffusion to one dimension. This is also supported by the increased presence of ciliary proteins along the IFs in the ciliary mutants *daf-25* and *daf-19* (Figs 6, 7). Time-lapse analysis of protein trafficking along IFs could be used to test this potential role of these structures in AFD neurons, but is beyond the scope of this study.

The requirement of ciliary proteins in cGMP signaling

We identified several ciliary proteins that are needed for proper localization of cGMP signaling components. Besides mediating the ciliary localization of DAF-11 (Jensen et al., 2010) and GCY-12 (Fujiwara et al., 2010), DAF-25 is also required for the proper localization of three other guanylyl cyclases in the AFD neurons, suggesting that DAF-25 is a general modulator of guanylyl cyclase localization in cilia. The *daf-25* mutation also results in defective finger formation (Fig. 6B). Given that photoreceptor degeneration is often associated with mislocalization of signaling proteins from the outer segment (Wheway et al., 2014), and that the mammalian ortholog Ankmy2 binds the photoreceptor GC1 (Jensen et al., 2010), we predict that mammalian Ankmy2 might play roles in ciliary photoreceptor development, function and degeneration.

The proper localization of guanylyl cyclases to fingers also requires BBS proteins in an IFT-independent manner (Fig. 6D,E), consistent with the apparent lack of IFT proteins and microtubules (required for IFT motility) in this compartment. Besides its function in IFT, the BBSome also facilitates vesicular trafficking of ciliary proteins at the base of cilia (Nachury et al., 2007); such a function could also potentially be carried out at the ring structure, which is where vesicles likely dock before membrane proteins disperse into the finger area, and more distally, the cilium. Disruption of BBS proteins has been reported to result in mislocalization of GPCRs (Berbari et al., 2008; Domire et al., 2011), but this is the first time that BBS proteins have been reported to be involved specifically in the trafficking of guanylyl cyclases, a central component of cGMP signaling. Our finding that only guanylyl cyclase localization is affected in both *bbs* and *daf-25* mutants provides evidence that the trafficking of guanylyl cyclases is an important step in the regulation of cGMP signaling by ciliary proteins.

We showed that NPHP-2/inversin colocalizes with the CNG channel subunit TAX-4 and is required for its proper localization in the inversin compartment (Fig. 7). The altered localization of TAX-4 in the *nphp-2* mutant is similar to that reported in AWB neurons by Wojtyniak et al. (Wojtyniak et al., 2013), but milder than the phenotype seen in mammalian inversin mutant cells (Shiba et al., 2010). In *nphp-2* mutant worms, the encoded protein is predicted to still localize to the inversin compartment given that the C-terminal region, required for proper localization, is intact (Shiba et al., 2009), but might have a reduced ability to interact with binding partners due to the missing ankyrin repeats. Thus, the truncated NPHP-2 might have reduced affinity for TAX-4 (directly or indirectly), leading to TAX-4 leakage into the distal part of the cilium and a thermotaxis phenotype. Understanding the basis of this defect will be of interest, as it might, for example, help shed light on the role of mammalian NPHP2/inversin and the 'inversin compartment' that play essential roles in Wnt signaling (Lienkamp et al., 2012).

The ciliary mutants tested have various protein mislocalization patterns, but all are expected to result in defective sensory transduction through the misregulation of key signaling components (Fig. 8B). Notably, defective signaling could result in mutant phenotypes that are different from those arising from a complete lack of signaling proteins. Our thermotaxis data suggest that mislocalized signaling proteins could lead to defective behaviors (supplementary material Fig. S4). However, because of the involvement of AFD and other neurons in both thermosensation and locomotion – two components of the themotaxis behavior – additional studies will be required to uncover how the mislocalization of cGMP signaling proteins in the AFD neurons of ciliary mutants might result in their thermotaxis and/or movement phenotypes. Finally, given the close relationship between AFD neurons and vertebrate photoreceptors, which also partition cGMP signaling machinery on distinct membranes, our findings might help provide insights into the mechanism of normal retinal function and degeneration in the context of ciliopathies.

MATERIALS AND METHODS

Strains

All strains were cultured at 20℃ using standard techniques (Brenner, 1974). The Bristol strain N2 was used as the wild type. The mutant strains used were MX52 *bbs-8(nx77)*, MX972 *daf-25(m362); daf-12(sa204)*, JT6924*daf-19(m86); daf-12(sa204)*, JT204 *daf-12(sa204)*, MT3645 *bbs-7(n1606)*, PR813 *osm-5(p813)*, CB3330 *che-11(e1810)*, MX1331 *nphp-2(gk653)*, MX754 *mks-5(tm3100)*. The *daf-25* and *daf-19* mutants were used in the context of *daf-12* background to suppress the developmental arrest (dauer) of the *daf-25* and *daf-19* mutants, with the *daf-12* mutant alone showing a normal phenotype. A list of transgenic strains is available upon request.

Construction of transgenic strains

Translational fluorescent fusion constructs were created by stitch PCR (Hobert, 2002). The AFD-specific constructs were made by using the 1.5-kb upstream region of the *gcy-8* gene as the promoter. Templates for PCR amplification were either genomic DNA from N2, or plasmids *p328* (*osm-5::xbx-1::tdTomato*), *p344* (*nphp-1::tdTomato*), *p342.1* (*osm-5::mks-6::gfp*) – gifts from Bradley Yoder, University of Alabama, AL. Constructs were injected at the 5–10 ng/µl range.

Microscopy

Live animals were anaesthetized with 10 mM levamisole, mounted on 5% agarose pads with 0.1-µm-diameter polystyrene beads (Polysciences, PA), and observed under epifluorescence or spinning disk confocal microscopes. Image analyses were carried out using Volocity (Improvision) for deconvolution and colocalization.

Electron tomography

Animals were prepared by high-pressure freezing, using a Bal-tech HM 010 High Pressure Freezer, followed by freeze substitution into osmium fixative in 100% acetone in an RMC Freeze Substitution Device. After warming to 0℃, samples were washed in 100% acetone and embedded into Embed-812 resin. Semi-thick serial sections were collected onto Pioloform-coated slot grids, and viewed on an FEI Technai F20 electron microscope. Tomograms were calculated using a back-projection method using internal reference points (‘markerless alignment’) (Hall et al., 2012). The three-dimensional reconstruction of electron tomograms was performed using IMOD software. One tomogram consists of 1256 serial levels after combining dual-axis tomograms from 15 serial thick sections.

Acknowledgements

Mutant strains were provided by the Caenorhabditis Genetics Center (CGC). Electron tomography was conducted at the New York Structural Biology Center, with technical help from Ken Nguyen, William J. Rice, Laura X. Williams and Kevin Fisher, and financial support from the Albert Einstein College of Medicine. We thank Ed Hedgecock for access to archival TEM data from wild-type adults that was first generated for Perkins et al. (Perkins et al., 1986); those images are now available at www.wormimage.org, with support from National Institutes of Health (OD 010943 to D.H.H.).

Competing interests

The authors declare no competing interests.

Author contributions

P.A.T.N., D.H.H. and M.R.L. conceived of and designed the study, analyzed and interpreted data, and prepared the manuscript; P.A.T.N. carried out all experiments except for the electron tomography, which was performed by W.L.

Funding

M.R.L acknowledges funding from the Canadian Institutes of Health Research (CIHR) [grant number CBM201273]; March of Dimes; and the Michael Smith Foundation for Health Research (MSFHR) for a senior scholar award. D.H.H. acknowledges funding from the National Institutes of Health [grant number OD010943]. P.A.N acknowledges a graduate scholarship from CIHR. Deposited in PMC for release after 12 months.

Supplementary material

Supplementary material available online at
http://jcs.biologists.org/lookup/suppl/doi:10.1242/jcs.157610/-/DC1

References

Adams, N. A., Awadein, A. and Toma, H. S. (2007). The retinal ciliopathies. *Ophthalmic Genet.* **28**, 113-125.

Aveldaño, M. I. and Bazán, N. G. (1983). Molecular species of phosphatidylcholine, -ethanolamine, -serine, and -inositol in microsomal and photoreceptor membranes of bovine retina. *J. Lipid Res.* **24**, 620-627.

Badano, J. L., Mitsuma, N., Beales, P. L. and Katsanis, N. (2006). The ciliopathies: an emerging class of human genetic disorders. *Annu. Rev. Genomics Hum. Genet.* **7**, 125-148.

Bae, Y.-K., Qin, H., Knobel, K. M., Hu, J., Rosenbaum, J. L. and Barr, M. M. (2006). General and cell-type specific mechanisms target TRPP2/PKD-2 to cilia. *Development* **133**, 3859-3870.

Beales, P. L., Elcioglu, N., Woolf, A. S., Parker, D. and Flinter, F. A. (1999). New criteria for improved diagnosis of Bardet-Biedl syndrome: results of a population survey. *J. Med. Genet.* **36**, 437-446.

Berbari, N. F., Lewis, J. S., Bishop, G. A., Askwith, C. C. and Mykytyn, K. (2008). Bardet-Biedl syndrome proteins are required for the localization of G protein-coupled receptors to primary cilia. *Proc. Natl. Acad. Sci. USA* **105**, 4242-4246.

Berbari, N. F., O'Connor, A. K., Haycraft, C. J. and Yoder, B. K. (2009). The primary cilium as a complex signaling center. *Curr. Biol.* **19**, R526-R535.

Beverly, M., Anbil, S. and Sengupta, P. (2011). Degeneracy and neuromodulation among thermosensory neurons contribute to robust thermosensory behaviors in Caenorhabditis elegans. *J. Neurosci.* **31**, 11718-11727.

Biron, D., Shibuya, M., Gabel, C., Wasserman, S. M., Clark, D. A., Brown, A., Sengupta, P. and Samuel, A. D. T. (2006). A diacylglycerol kinase modulates long-term thermotactic behavioral plasticity in C. elegans. *Nat. Neurosci.* **9**, 1499-1505.

Biron, D., Wasserman, S., Thomas, J. H., Samuel, A. D. T. and Sengupta, P. (2008). An olfactory neuron responds stochastically to temperature and modulates Caenorhabditis elegans thermotactic behavior. *Proc. Natl. Acad. Sci. USA* **105**, 11002-11007.

Blacque, O. E., Reardon, M. J., Li, C., McCarthy, J., Mahjoub, M. R., Ansley, S. J., Badano, J. L., Mah, A. K., Beales, P. L., Davidson, W. S. et al. (2004). Loss of C. elegans BBS-7 and BBS-8 protein function results in cilia defects and compromised intraflagellar transport. *Genes Dev.* **18**, 1630-1642.

Boesze-Battaglia, K. and Schimmel, R. (1997). Cell membrane lipid composition and distribution: implications for cell function and lessons learned from photoreceptors and platelets. *J. Exp. Biol.* **200**, 2927-2936.

Brenner, S. (1974). The genetics of Caenorhabditis elegans. *Genetics* **77**, 71-94.

Cevik, S., Hori, Y., Kaplan, O. I., Kida, K., Toivenon, T., Foley-Fisher, C., Cottell, D., Katada, T., Kontani, K. and Blacque, O. E. (2010). Joubert syndrome Arl13b functions at ciliary membranes and stabilizes protein transport in Caenorhabditis elegans. *J. Cell Biol.* **188**, 953-969.

Choksi, S. P., Lauter, G., Swoboda, P. and Roy, S. (2014). Switching on cilia: transcriptional networks regulating ciliogenesis. *Development* **141**, 1427-1441.

Clark, D. A., Biron, D., Sengupta, P. and Samuel, A. D. T. (2006). The AFD sensory neurons encode multiple functions underlying thermotactic behavior in Caenorhabditis elegans. *J. Neurosci.* **26**, 7444-7451.

Coburn, C. M. and Bargmann, C. I. (1996). A putative cyclic nucleotide-gated channel is required for sensory development and function in C. elegans. *Neuron* **17**, 695-706.

Colosimo, M. E., Brown, A., Mukhopadhyay, S., Gabel, C., Lanjuin, A. E., Samuel, A. D. T. and Sengupta, P. (2004). Identification of thermosensory and olfactory neuron-specific genes via expression profiling of single neuron types. *Curr. Biol.* **14**, 2245-2251.

Corbit, K. C., Aanstad, P., Singla, V., Norman, A. R., Stainier, D. Y. R. and Reiter, J. F. (2005). Vertebrate Smoothened functions at the primary cilium. *Nature* **437**, 1018-1021.

Craige, B., Tsao, C.-C., Diener, D. R., Hou, Y., Lechtreck, K.-F., Rosenbaum, J. L. and Witman, G. B. (2010). CEP290 tethers flagellar transition zone microtubules to the membrane and regulates flagellar protein content. *J. Cell Biol.* **190**, 927-940.

daCosta, C. J. B. and Baenziger, J. E. (2009). A lipid-dependent uncoupled conformation of the acetylcholine receptor. *J. Biol. Chem.* **284**, 17819-17825.

Domire, J. S., Green, J. A., Lee, K. G., Johnson, A. D., Askwith, C. C. and Mykytyn, K. (2011). Dopamine receptor 1 localizes to neuronal cilia in a dynamic process that requires the Bardet-Biedl syndrome proteins. *Cell. Mol. Life Sci.* **68**, 2951-2960.

Donaldson, J. C., Dempsey, P. J., Reddy, S., Bouton, A. H., Coffey, R. J. and Hanks, S. K. (2000). Crk-associated substrate p130(Cas) interacts with nephrocystin and both proteins localize to cell-cell contacts of polarized epithelial cells. *Exp. Cell Res.* **256**, 168-178.

Doroquez, D. B., Berciu, C., Anderson, J. R., Sengupta, P. and Nicastro, D. (2014). A high-resolution morphological and ultrastructural map of anterior sensory cilia and glia in Caenorhabditis elegans. *Elife* **3**, e01948.

Erclik, T., Hartenstein, V., McInnes, R. R. and Lipshitz, H. D. (2009). Eye evolution at high resolution: the neuron as a unit of homology. *Dev. Biol.* **332**, 70-79.

Forte, M., Satow, Y., Nelson, D. and Kung, C. (1981). Mutational alteration of membrane phospholipid composition and voltage-sensitive ion channel function in paramecium. *Proc. Natl. Acad. Sci.* **78**, 7195-7199.

Fujiwara, M., Sengupta, P. and McIntire, S. L. (2002). Regulation of body size and behavioral state of C. elegans by sensory perception and the EGL-4 cGMP-dependent protein kinase. *Neuron* **36**, 1091-1102.

Fujiwara, M., Teramoto, T., Ishihara, T., Ohshima, Y. and McIntire, S. L. (2010). A novel zf-MYND protein, CHB-3, mediates guanylyl cyclase localization to sensory cilia and controls body size of Caenorhabditis elegans. *PLoS Genet.* **6**, e1001211.

Garcia-Gonzalo, F. R., Corbit, K. C., Sirerol-Piquer, M. S., Ramaswami, G., Otto, E. A., Noriega, T. R., Seol, A. D., Robinson, J. F., Bennett, C. L., Josifova, D. J. et al. (2011). A transition zone complex regulates mammalian ciliogenesis and ciliary membrane composition. *Nat. Genet.* **43**, 776-784.

Gray, J. M., Hill, J. J. and Bargmann, C. I. (2005). A circuit for navigation in Caenorhabditis elegans. *Proc. Natl. Acad. Sci. USA* **102**, 3184-3191.

Hall, D. H., Hartwieg, E. and Nguyen, K. C. Q. (2012). Modern electron microscopy methods for C. elegans. *Methods Cell Biol.* **107**, 93-149.

Hedgecock, E. M. and Russell, R. L. (1975). Normal and mutant thermotaxis in the nematode Caenorhabditis elegans. *Proc. Natl. Acad. Sci. USA* **72**, 4061-4065.
Hobert, O. (2002). PCR fusion-based approach to create reporter gene constructs for expression analysis in transgenic C. elegans. *Biotechniques* **32**, 728-730.
Huang, L., Szymanska, K., Jensen, V. L., Janecke, A. R., Innes, A. M., Davis, E. E., Frosk, P., Li, C., Willer, J. R., Chodirker, B. N. et al. (2011). TMEM237 is mutated in individuals with a Joubert syndrome related disorder and expands the role of the TMEM family at the ciliary transition zone. *Am. J. Hum. Genet.* **89**, 713-730.
Inada, H., Ito, H., Satterlee, J., Sengupta, P., Matsumoto, K. and Mori, I. (2006). Identification of guanylyl cyclases that function in thermosensory neurons of Caenorhabditis elegans. *Genetics* **172**, 2239-2252.
Insinna, C. and Besharse, J. C. (2008). Intraflagellar transport and the sensory outer segment of vertebrate photoreceptors. *Dev. Dyn.* **237**, 1982-1992.
Jensen, V. L., Bialas, N. J., Bishop-Hurley, S. L., Molday, L. L., Kida, K., Nguyen, P. A. T., Blacque, O. E., Molday, R. S., Leroux, M. R. and Riddle, D. L. (2010). Localization of a guanylyl cyclase to chemosensory cilia requires the novel ciliary MYND domain protein DAF-25. *PLoS Genet.* **6**, e1001199.
Jin, H., White, S. R., Shida, T., Schulz, S., Aguiar, M., Gygi, S. P., Bazan, J. F. and Nachury, M. V. (2010). The conserved Bardet-Biedl syndrome proteins assemble a coat that traffics membrane proteins to cilia. *Cell* **141**, 1208-1219.
Johnson, J.-L. F. and Leroux, M. R. (2010). cAMP and cGMP signaling: sensory systems with prokaryotic roots adopted by eukaryotic cilia. *Trends Cell Biol.* **20**, 435-444.
Kaplan, M. R., Cho, M. H., Ullian, E. M., Isom, L. L., Levinson, S. R. and Barres, B. A. (2001). Differential control of clustering of the sodium channels Na(v)1.2 and Na(v)1.6 at developing CNS nodes of Ranvier. *Neuron* **30**, 105-119.
Kaplan, O. I., Doroquez, D. B., Cevik, S., Bowie, R. V., Clarke, L., Sanders, A. A. W. M., Kida, K., Rappoport, J. Z., Sengupta, P. and Blacque, O. E. (2012). Endocytosis genes facilitate protein and membrane transport in C. elegans sensory cilia. *Curr. Biol.* **22**, 451-460.
Komatsu, H., Mori, I., Rhee, J. S., Akaike, N. and Ohshima, Y. (1996). Mutations in a cyclic nucleotide-gated channel lead to abnormal thermosensation and chemosensation in C. elegans. *Neuron* **17**, 707-718.
Köppen, M., Simske, J. S., Sims, P. A., Firestein, B. L., Hall, D. H., Radice, A. D., Rongo, C. and Hardin, J. D. (2001). Cooperative regulation of AJM-1 controls junctional integrity in Caenorhabditis elegans epithelia. *Nat. Cell Biol.* **3**, 983-991.
Kuhara, A., Inada, H., Katsura, I. and Mori, I. (2002). Negative regulation and gain control of sensory neurons by the C. elegans calcineurin TAX-6. *Neuron* **33**, 751-763.
Kuhara, A., Okumura, M., Kimata, T., Tanizawa, Y., Takano, R., Kimura, K. D., Inada, H., Matsumoto, K. and Mori, I. (2008). Temperature sensing by an olfactory neuron in a circuit controlling behavior of C. elegans. *Science* **320**, 803-807.
Lienkamp, S., Ganner, A. and Walz, G. (2012). Inversin, Wnt signaling and primary cilia. *Differ. Res. Biol. Divers.* **83**, S49-S55.
Menco, B. P. (1997). Ultrastructural aspects of olfactory signaling. *Chem. Senses* **22**, 295-311.
Mok, C. A., Healey, M. P., Shekhar, T., Leroux, M. R., Héon, E. and Zhen, M. (2011). Mutations in a guanylate cyclase GCY-35/GCY-36 modify Bardet-Biedl syndrome-associated phenotypes in Caenorhabditis elegans. *PLoS Genet.* **7**, e1002335.
Mollet, G., Silbermann, F., Delous, M., Salomon, R., Antignac, C. and Saunier, S. (2005). Characterization of the nephrocystin/nephrocystin-4 complex and subcellular localization of nephrocystin-4 to primary cilia and centrosomes. *Hum. Mol. Genet.* **14**, 645-656.
Mori, I. and Ohshima, Y. (1995). Neural regulation of thermotaxis in Caenorhabditis elegans. *Nature* **376**, 344-348.
Mukhopadhyay, S., Lu, Y., Shaham, S. and Sengupta, P. (2008). Sensory signaling-dependent remodeling of olfactory cilia architecture in C. elegans. *Dev. Cell* **14**, 762-774.
Nachury, M. V., Loktev, A. V., Zhang, Q., Westlake, C. J., Peränen, J., Merdes, A., Slusarski, D. C., Scheller, R. H., Bazan, J. F., Sheffield, V. C. et al. (2007). A core complex of BBS proteins cooperates with the GTPase Rab8 to promote ciliary membrane biogenesis. *Cell* **129**, 1201-1213.
Nishimura, D. Y., Fath, M., Mullins, R. F., Searby, C., Andrews, M., Davis, R., Andorf, J. L., Mykytyn, K., Swiderski, R. E., Yang, B. et al. (2004). Bbs2-null mice have neurosensory deficits, a defect in social dominance, and retinopathy associated with mislocalization of rhodopsin. *Proc. Natl. Acad. Sci. USA* **101**, 16588-16593.
Okochi, Y., Kimura, K. D., Ohta, A. and Mori, I. (2005). Diverse regulation of sensory signaling by C. elegans nPKC-epsilon/eta TTX-4. *EMBO J.* **24**, 2127-2137.
Ou, G., Blacque, O. E., Snow, J. J., Leroux, M. R. and Scholey, J. M. (2005). Functional coordination of intraflagellar transport motors. *Nature* **436**, 583-587.
Ou, G., Koga, M., Blacque, O. E., Murayama, T., Ohshima, Y., Schafer, J. C., Li, C., Yoder, B. K., Leroux, M. R. and Scholey, J. M. (2007). Sensory ciliogenesis in Caenorhabditis elegans: assignment of IFT components into distinct modules based on transport and phenotypic profiles. *Mol. Biol. Cell* **18**, 1554-1569.
Perkins, L. A., Hedgecock, E. M., Thomson, J. N. and Culotti, J. G. (1986). Mutant sensory cilia in the nematode Caenorhabditis elegans. *Dev. Biol.* **117**, 456-487.
Poo, M. and Cone, R. A. (1974). Lateral diffusion of rhodopsin in the photoreceptor membrane. *Nature* **247**, 438-441.
Potokar, M., Kreft, M., Li, L., Daniel Andersson, J., Pangrsic, T., Chowdhury, H. H., Pekny, M. and Zorec, R. (2007). Cytoskeleton and vesicle mobility in astrocytes. *Traffic* **8**, 12-20.
Reiter, J. F., Blacque, O. E. and Leroux, M. R. (2012). The base of the cilium: roles for transition fibres and the transition zone in ciliary formation, maintenance and compartmentalization. *EMBO Rep.* **13**, 608-618.
Rosenbaum, J. L. and Witman, G. B. (2002). Intraflagellar transport. *Nat. Rev. Mol. Cell Biol.* **3**, 813-825.
Ruppersburg, C. C. and Hartzell, H. C. (2014). The Ca2+-activated Cl- channel ANO1/TMEM16A regulates primary ciliogenesis. *Mol. Biol. Cell* **25**, 1793-1807.
Sang, L., Miller, J. J., Corbit, K. C., Giles, R. H., Brauer, M. J., Otto, E. A., Baye, L. M., Wen, X., Scales, S. J., Kwong, M. et al. (2011). Mapping the NPHP-JBTS-MKS protein network reveals ciliopathy disease genes and pathways. *Cell* **145**, 513-528.
Schafer, J. C., Haycraft, C. J., Thomas, J. H., Yoder, B. K. and Swoboda, P. (2003). XBX-1 encodes a dynein light intermediate chain required for retrograde intraflagellar transport and cilia assembly in Caenorhabditis elegans. *Mol. Biol. Cell* **14**, 2057-2070.
Schmidt, D., Jiang, Q.-X. and MacKinnon, R. (2006). Phospholipids and the origin of cationic gating charges in voltage sensors. *Nature* **444**, 775-779.
Schneider, L., Clement, C. A., Teilmann, S. C., Pazour, G. J., Hoffmann, E. K., Satir, P. and Christensen, S. T. (2005). PDGFRalphaalpha signaling is regulated through the primary cilium in fibroblasts. *Curr. Biol.* **15**, 1861-1866.
Sedmak, T. and Wolfrum, U. (2011). Intraflagellar transport proteins in ciliogenesis of photoreceptor cells. *Biol. Cell* **103**, 449-466.
Shiba, D., Yamaoka, Y., Hagiwara, H., Takamatsu, T., Hamada, H. and Yokoyama, T. (2009). Localization of Inv in a distinctive intraciliary compartment requires the C-terminal ninein-homolog-containing region. *J. Cell Sci.* **122**, 44-54.
Shiba, D., Manning, D. K., Koga, H., Beier, D. R. and Yokoyama, T. (2010). Inv acts as a molecular anchor for Nphp3 and Nek8 in the proximal segment of primary cilia. *Cytoskeleton (Hoboken)* **67**, 112-119.
Silverman, M. A. and Leroux, M. R. (2009). Intraflagellar transport and the generation of dynamic, structurally and functionally diverse cilia. *Trends Cell Biol.* **19**, 306-316.
Simons, M., Gloy, J., Ganner, A., Bullerkotte, A., Bashkurov, M., Krönig, C., Schermer, B., Benzing, T., Cabello, O. A., Jenny, A. et al. (2005). Inversin, the gene product mutated in nephronophthisis type II, functions as a molecular switch between Wnt signaling pathways. *Nat. Genet.* **37**, 537-543.
Styers, M. L., Kowalczyk, A. P. and Faundez, V. (2005). Intermediate filaments and vesicular membrane traffic: the odd couple's first dance? *Traffic* **6**, 359-365.
Sulston, J. E., Schierenberg, E., White, J. G. and Thomson, J. N. (1983). The embryonic cell lineage of the nematode Caenorhabditis elegans. *Dev. Biol.* **100**, 64-119.
Sung, C. H. and Leroux, M. R. (2013). The roles of evolutionarily conserved functional modules in cilia-related trafficking. *Nat. Cell Biol.* **15**, 1387-1397.
Swoboda, P., Adler, H. T. and Thomas, J. H. (2000). The RFX-type transcription factor DAF-19 regulates sensory neuron cilium formation in C. elegans. *Mol. Cell* **5**, 411-421.
Tan, P. L., Barr, T., Inglis, P. N., Mitsuma, N., Huang, S. M., Garcia-Gonzalez, M. A., Bradley, B. A., Coforio, S., Albrecht, P. J., Watnick, T. et al. (2007). Loss of Bardet Biedl syndrome proteins causes defects in peripheral sensory innervation and function. *Proc. Natl. Acad. Sci. USA* **104**, 17524-17529.
Warburton-Pitt, S. R. F., Jauregui, A. R., Li, C., Wang, J., Leroux, M. R. and Barr, M. M. (2012). Ciliogenesis in Caenorhabditis elegans requires genetic interactions between ciliary middle segment localized NPHP-2 (inversin) and transition zone-associated proteins. *J. Cell Sci.* **125**, 2592-2603.
Weinshenker, D., Wei, A., Salkoff, L. and Thomas, J. H. (1999). Block of an ether-a-go-go-like K(+) channel by imipramine rescues egl-2 excitation defects in Caenorhabditis elegans. *J. Neurosci.* **19**, 9831-9840.
Wheway, G., Parry, D. A. and Johnson, C. A. (2014). The role of primary cilia in the development and disease of the retina. *Organogenesis* **10**, 69-85.
Williams, C. L., Li, C., Kida, K., Inglis, P. N., Mohan, S., Semenec, L., Bialas, N. J., Stupay, R. M., Chen, N., Blacque, O. E. et al. (2011). MKS and NPHP modules cooperate to establish basal body/transition zone membrane associations and ciliary gate function during ciliogenesis. *J. Cell Biol.* **192**, 1023-1041.
Wojtyniak, M., Brear, A. G., O'Halloran, D. M. and Sengupta, P. (2013). Cell- and subunit-specific mechanisms of CNG channel ciliary trafficking and localization in C. elegans. *J. Cell Sci.* **126**, 4381-4395.
Yu, S., Avery, L., Baude, E. and Garbers, D. L. (1997). Guanylyl cyclase expression in specific sensory neurons: a new family of chemosensory receptors. *Proc. Natl. Acad. Sci. USA* **94**, 3384-3387.
Zacharias, D. A., Violin, J. D., Newton, A. C. and Tsien, R. Y. (2002). Partitioning of lipid-modified monomeric GFPs into membrane microdomains of live cells. *Science* **296**, 913-916.